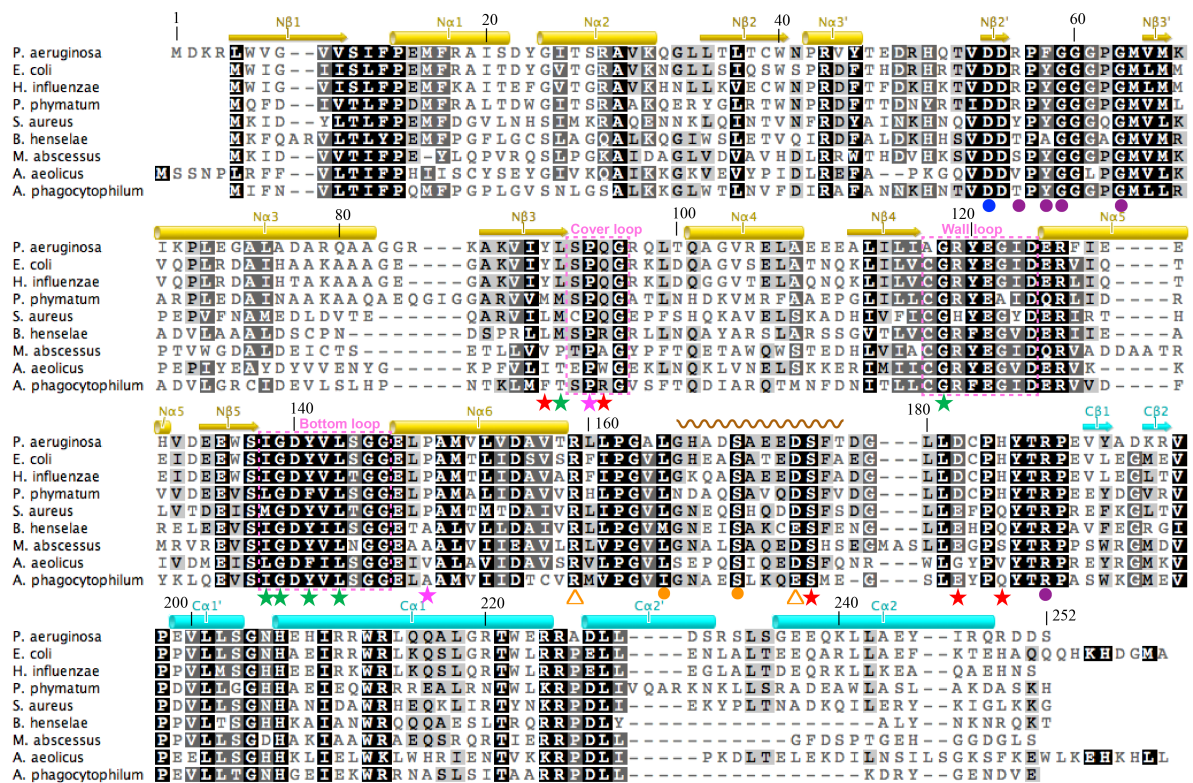
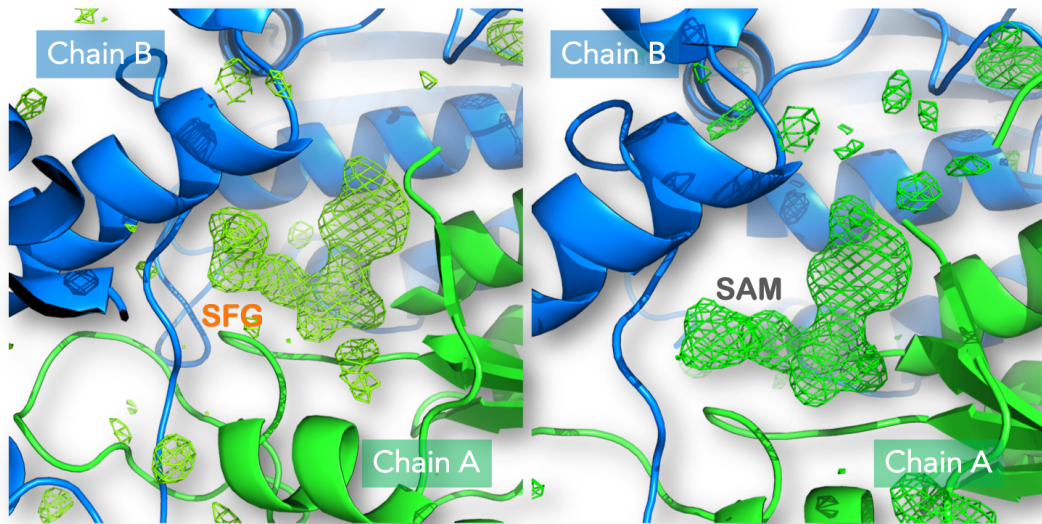


Supplemental Figure S1. Overview of *PaTrmD* homodimer bound to SAM. (A, B) Two orthogonal views of *PaTrmD*-SAM structure showing the dimer architecture and SAM-binding active site. The polypeptide chain is shown as a cartoon. Bound SAM molecules are represented by spheres. (C) Close-up of the domain arrangement and active site of *PaTrmD*. Each subunit of the *PaTrmD* dimer contains two domains: N-terminal domain harbouring the active site (NTD, residues 1-165) in yellow, and C-terminal domain (CTD, residues 178-252) in cyan. The linker loop or “lid” (residues 166-177) between NTD and CTD is unstructured in *PaTrmD*-SAM and its likely path is indicated by a red dotted line. Bound SAM is shown as magenta sticks with an unbiased *F_o-F_c* electron density (grey) map contoured at 3.0 σ overlaid on the model. Three loops that are involved in substrate binding are coloured in black: “cover loop” (residues 93-96), “wall loop” (residues 117-124) and “bottom loop” (residues 138-146), following nomenclature proposed previously (Ito et al. 2015).

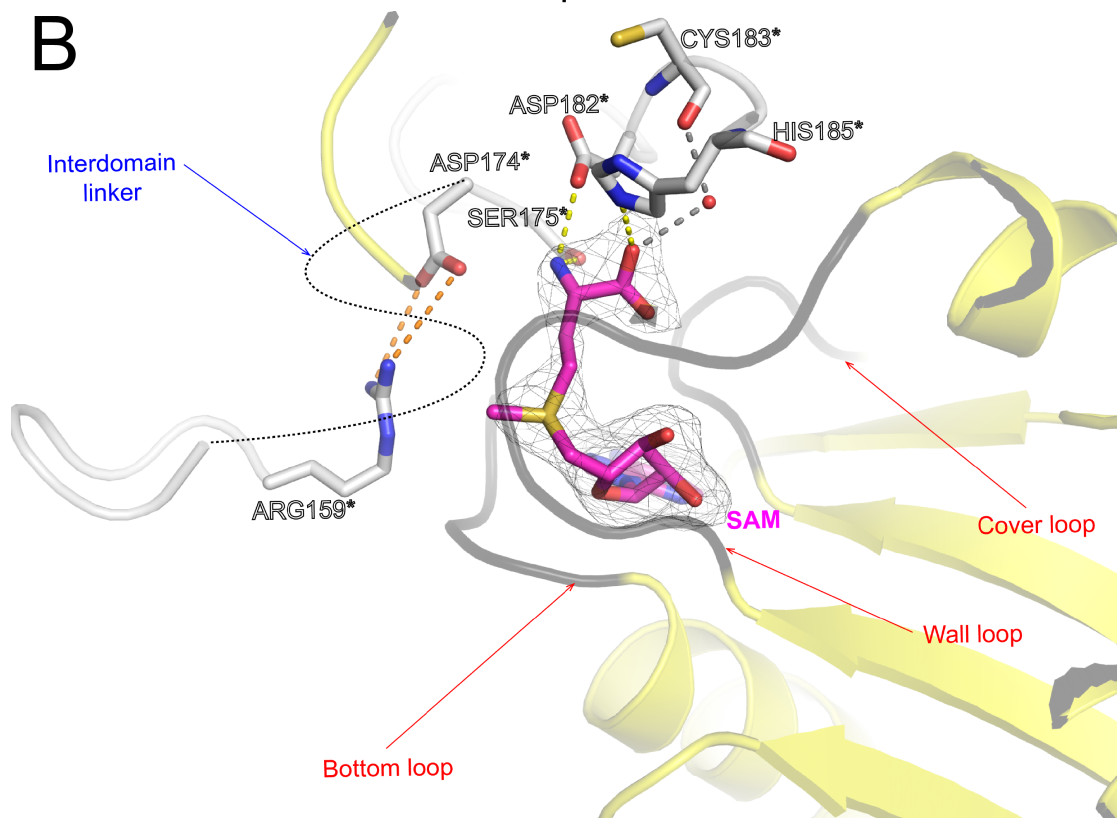
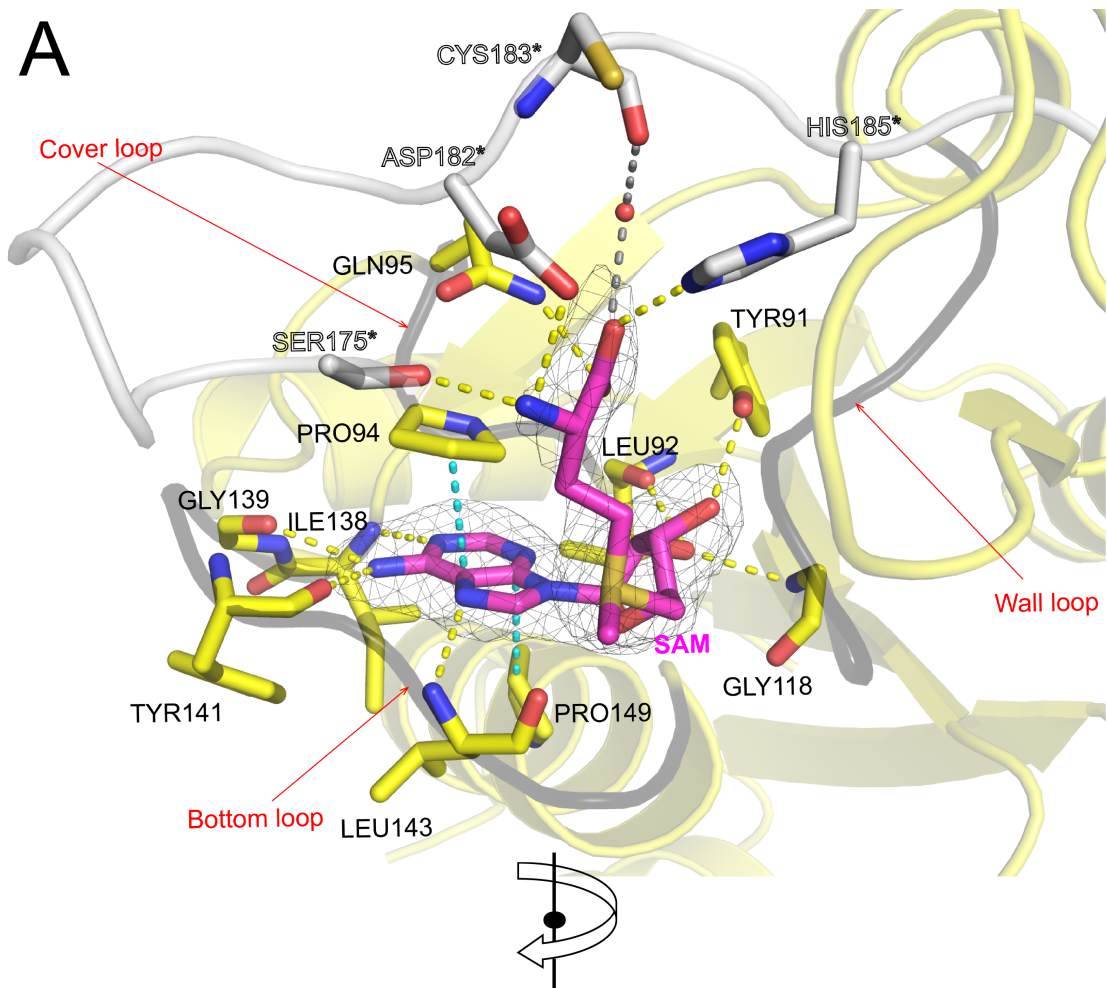
Ito T, Masuda I, Yoshida K, Goto-Ito S, Sekine S, Suh SW, Hou YM, Yokoyama S. 2015. Structural basis for methyl-donor-dependent and sequence-specific binding to tRNA substrates by knotted methyltransferase TrmD. *Proc Natl Acad Sci U S A* **112**: E4197-4205.



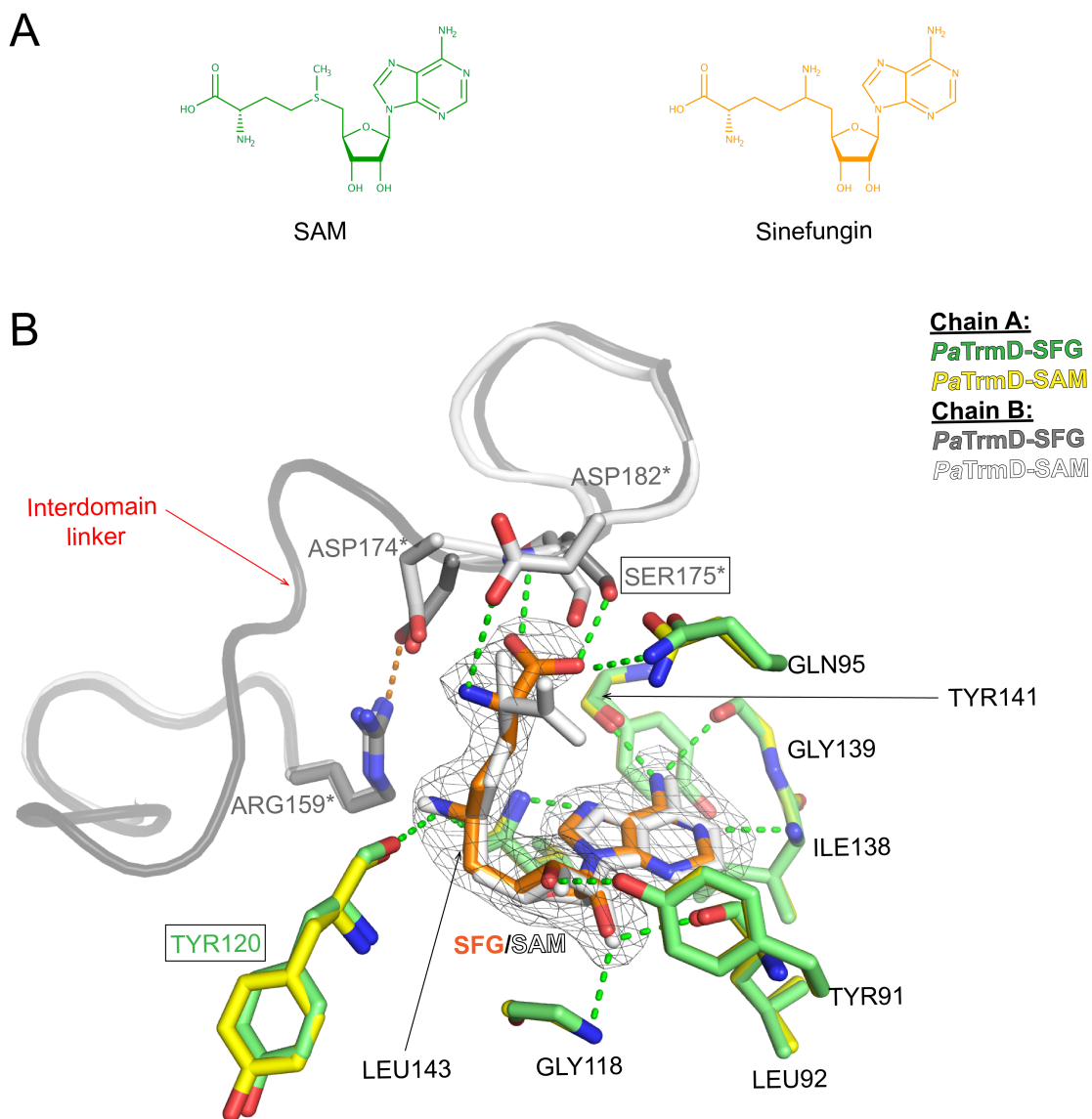
Supplemental Figure S2. Sequence alignment of TrmD orthologs. Amino acid sequences of TrmD from nine bacteria (*Pseudomonas aeruginosa*, *Escherichia coli*, *Haemophilus influenzae*, *Paraburkholderia phymatum*, *Staphylococcus aureus*, *Bartonella henselae*, *Mycobacterium abscessus*, *Aquifex aeolicus*, and *Anaplasma phagocytophilum*) were aligned by the program MUSCLE and visualized by the software Geneious. The level of amino acid conservation is indicated by shading from black (identical in eight or nine sequences) to grey (conserved in six or seven) to white (low or no conservation). Residue numbers corresponding to *Pa*TrmD are listed above the sequence. Secondary structural elements defined in *Pa*TrmD crystal structure are shown above the sequences (only α -helices and β -strands are shown). Secondary structural elements are labeled in different colors corresponding to their domain regions: N-terminal domain (NTD: yellow) and C-terminal domain (CTD: cyan). The flexible interdomain linker between NTD and CTD is indicated by wave line in brown color. Three active-site loops (cover loop, wall loop and bottom loop) are highlighted in magenta dashed box. In *Pa*TrmD, the amino acids involved in SAM binding are indicated by star in red (side-chain interacting), green (main-chain interacting), and magenta (stacking interacting), respectively. tRNA-interacting residues determined in *H. influenzae* structure (PDB ID: 4YVI) are highly conserved in the selected sequences and indicated by blue circle (G36-interacting), orange circles (G37-interacting) and purple (anti-codon branch-interacting), while G37-interacting catalytic residues are indicated by triangles.



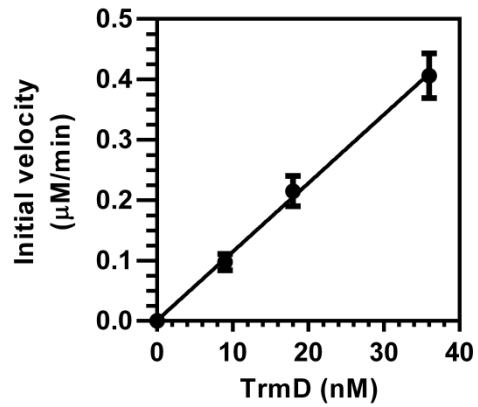
Supplemental Figure S3. The simulated annealing omit maps for SFG and SAM. The polypeptide chain is shown as a cartoon. Chain A of the *PaTrmD* dimer is colored green and chain B is colored blue. The maps for SFG and SAM are indicated.



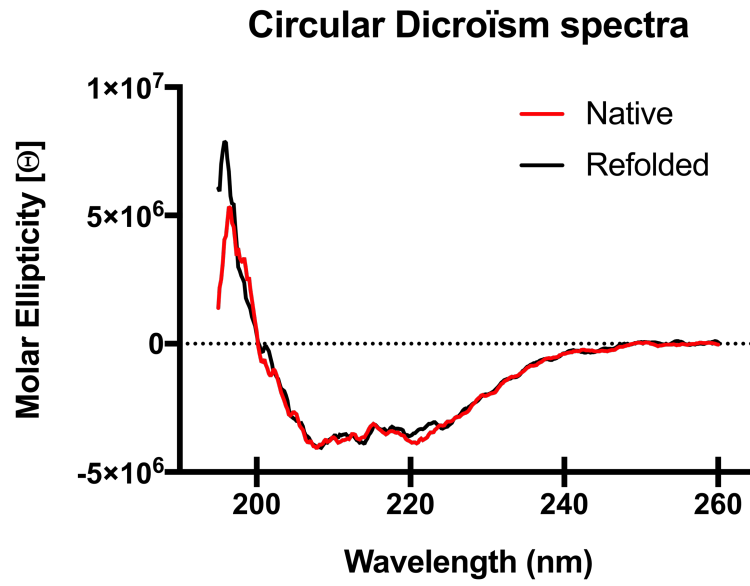
Supplemental Figure S4. The active site of *Pa*TrmD with bound SAM. (A) Close-up view of the active site showing the SAM-protein interactions. The polypeptide chain is shown as a cartoon with strands as arrows and helices are coils, whereas the residues involved in ligand binding are shown as sticks. Chain A of the *Pa*TrmD dimer is colored yellow and chain B is colored grey. Residues from Chain B are marked by asterisks. The SAM molecule is shown as a magenta stick. Water molecules are shown as red spheres. The omit *F_o-F_c* electron density for the SAM molecule is shown as a grey mesh contoured at 3.0 σ . Hydrogen bonds formed between *Pa*TrmD and SAM are indicated by yellow dashed lines while the stacking interactions are illustrated as cyan dashed lines. Cover loop, wall loop and bottom loop are highlighted in black. (B) Orthogonal view of (A) showing interface interactions. The unstructured interdomain linker in chain B (grey) is modeled as a black dotted line. The salt bridge formed between NTD and CTD is indicated as an orange dashed line.



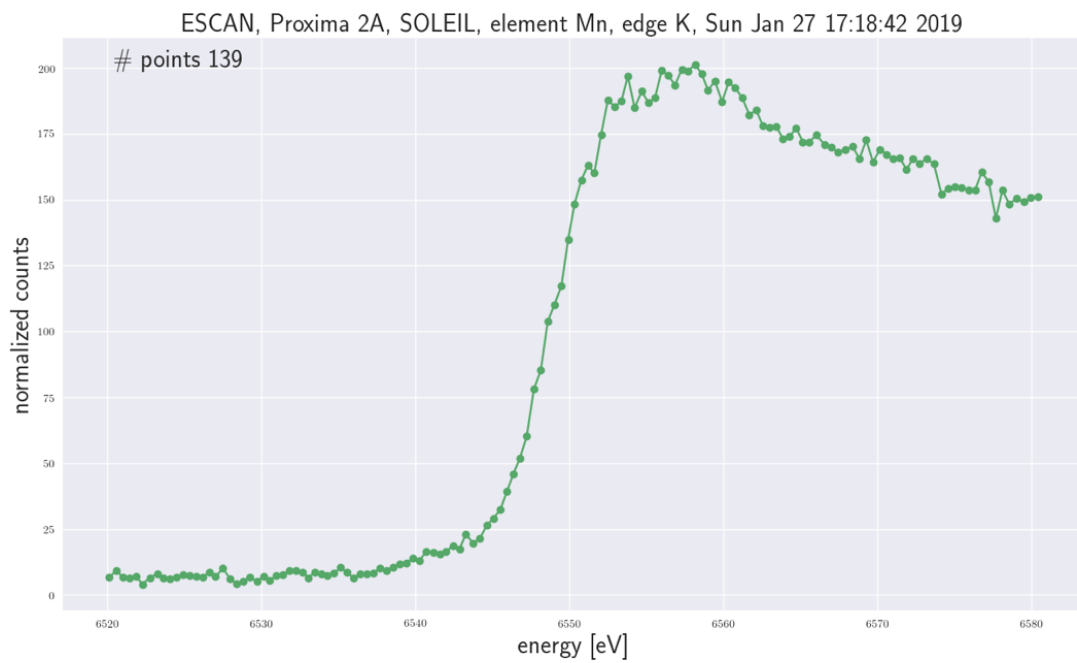
Supplemental Figure S5. Comparison of the binding modes of SAM and its analog SFG. (A) Chemical structures of SAM and sinefungin (SFG). (B) Active site of *PaTrmD-SFG* (green in chain A and grey in chain B) was superimposed on to the active site of *PaTrmD-SAM* (yellow in chain A and white in chain B) to compare the ligand-binding modes. Active-site ligands and the residues involved in ligand binding are shown as sticks. Loop regions (residues 159-182) in chain B containing the interdomain linker are shown as carton, where a salt bridge formed between ARG159 and ASP174 is indicated as an orange dashed line. Hydrogen bonds are shown as green dashed lines. Residues TYR120 and SER175 only form hydrogen bonds with SFG but not SAM. The stacking interactions between adenosine ring and proline residues (PRO94 and PRO149) are conserved in both structures but do not show in this figure to facilitate visualization. Residues from Chain B are marked by asterisks.



Supplemental Figure S6. The linear detection of the MTase-Glo with respect to initial velocity and concentration of *PaTrmD*. Reaction initial velocity was determined by varying the concentration of *PaTrmD* under the fixed concentration of tRNA^{Leu(GAG)} and SAM. *PaTrmD* concentrations in the reaction were varied from 0 to 100 nM. The data points represent mean \pm SD (n=3).



Supplemental Figure S7. The overlaid CD spectra of native *PaTrmD* and refolded *PaTrmD*.



Supplemental Figure S8. The anomalous absorption edge showing the absorption at K edge of manganese.